900 MHZ TO 1.5 GHZ SINGLE-ENDED CMOS MIXER FOR WIRELESS COMMUNICATION SYSTEMS

***Akwuruoha, C. N.**

Department of Electrical and Electronic Engineering Michael Okpara University of Agriculture, Umudike, Nigeria.

*Corresponding Author: akwuruoha.charles@mouau.edu.ng

ABSTRACT

This paper presents a 900 MHz to 1.5 GHz Single-ended CMOS Mixer for wireless communications systems. The Mixer was designed with Keysight Advanced Design System (ADS) Software based on BSIM_3 model nMOS and pMOS field effect transistors biased with drain supply voltage of 3V and gate voltage 0V. The Mixer was simulated for down-conversion and up-conversion. Harmonic Balance simulation was carried and the drain resistance (RD) of the Mixer was the parameter swept from 10 to 820 ohms. In the down-conversion, the radio frequency (RF) is the input port while the intermediate frequency (IF) is the output port. In the up-conversion, the IF is the input port while the RF is the output port. The RF frequency was swept from 900 MHz to 1.5 GHz. A Local oscillator (LO) to intermediate frequency (IF) isolation of 52.02 dB, an LO to RF isolation of 68.83 dB and RF to IF isolation of 16.57 dB were recorded at drain resistance of 410 Ω. Since the Mixer operational frequency ranges from 900 MHz to 1.5 GHz, the center frequency is 1.2 GHz. The results obtained at 1.2 GHz, indicates that the low and high third order intercept points are -8.54 dBm and 10.59 dBm respectively as well as transducer power gain of -25.63 dB. The lower sideband (LSB) and upper sideband (USB) IF power at 1.2 GHz are -55.63 dBm and -55.64 dBm respectively. The third order intermodulation power for LSB and USB at 1.2 GHz are -98.56 dBm and -136.86 dBm respectively.

Keywords: cmos; mixer; single-ended; radio frequency; local oscillator; intermediate frequency

1.0 INTRODUCTION

A mixer achieves frequency conversion with a three-port device having non-linear and time varying elements (Pozar, 2011). A mixer output is proportional to the product of its input signals such that operation of the mixer is dependent on the non-linearity of devices such as diode or transistor. Mixers such as sub- harmonic mixers have been discussed in some works (Marki and Marki, 2018); (Seyedhosseinzadeh and Nabavi, 2017); (Kishokumar *et al.,* 2017); (Wen *et al*., 2020); (Chen *et al*., 2016); (Chong *et al*,.2014); (Wang *et al.,* 2006); (Weng *et al*., 2007); (Mudjar and Musia,1993). Pozar (2011) also discussed that Mixer signals originate from two ports: radio frequency (input) port and local oscillator (LO) port as the output represents the intermediate frequency (IF) port. If the local oscillator frequency is denoted by f_{LO}, then the local oscillator signal (Pozar, 2011) is given by

$$V_{LO}(t) = \mathrm{Cos}2\pi f_{LO}t \qquad (1)$$

In this paper, up-conversion and down-conversion mixers and the respective spectra are considered and shown in Figures 1, 2, 3 and 4.

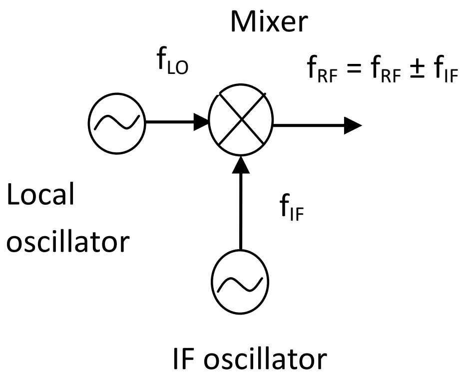

Figure 1: Mixer Frequency Up Conversion

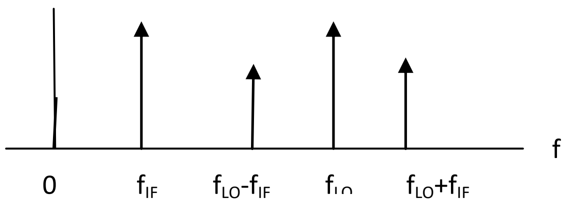

Figure 2: Mixer Up conversion Signal Spectra

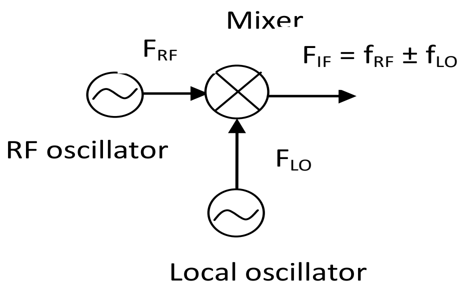

Figure 3: Mixer frequency Down Conversion

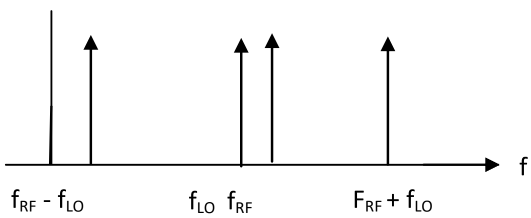

Figure 4: Mixture down conversion spectra

The transmitted signal when the intermediate frequency is one of the input signals is given by

$$V_{IF}(t) = \text{Cos}2\pi f_{IF}t \quad (2)$$

If the product of the mixer normal operation is a combination of local oscillator signal and intermediate frequency, the radio frequency (RF) signal is given by

$$V_{RF}(t) = KV_{LO}(t)V_{IF}(t) = KCos2\pi_{LO}tCos2\pi f_{IF}t \quad (3)$$

$$= K/2\ [Cos2\pi\ (f_{LO}-f_{IF})t + Cos2\pi(f_{LO}+f_{IF})t] \quad (4)$$

where the constant K is the voltage conversion loss of the mixer.

According to Pozar (2011), the upper sideband (USB) and lower sideband (LSB) RF signal consists of the sum and differences of the local oscillator (LO) frequency and intermediate frequency (IF) given by (5)

$$f_{RF} = f_{LO} \pm f_{IF} \quad (5)$$

where f_{RF} is radio frequency
f_{LO} is local oscillator frequency
f_{IF} is intermediate frequency

The mixer therefore modulates the local oscillator (LO) signal with the intermediate frequency (IF) signal. Equation (5) indicates the upper sideband (USB) and lower side band (LSB) signals are such that the USB is given by

$$USB = f_{LO} + f_{IF} \quad (6)$$

While the LSB is given by

$$LSB = f_{LO} - f_{IF} \quad (7)$$

2.0 DESIGN

Resonance circuit constitutes an important unit of the circuitry of a mixer. Resonance circuits have been discussed in some works (Yang *et al*., 2005); (Danndsena & Jena, 2022); (Boeck *et al*., 2010); (Lugo-Hernandez *et al*., 2023); (Lin *et al*. 2003); (Pozar, 2011). In this paper, a series resonance has been used to illustrate the behaviour of the resonator in the local oscillator section (LO) of the Mixer.

2.1 Series Resonance Circuit

A series resonance circuit is needed to provide resonance in the Mixer as described in Figure 5.

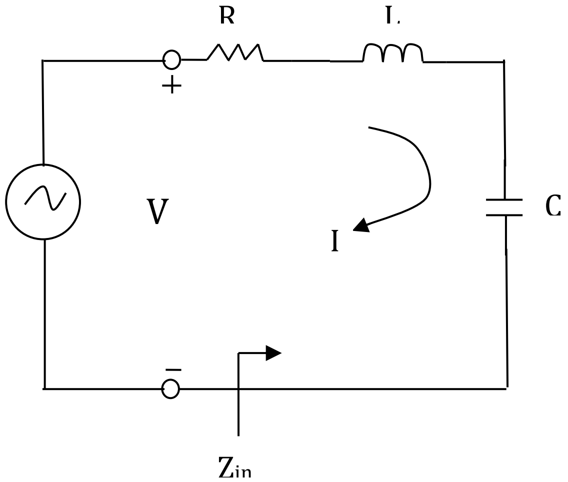

Figure 5: Series Resonance Circuit

The input impedance Z_{in} is given by

$$Z_{in} = j\omega L - 1/j\omega C \tag{6}$$

The complex power delivered to the resonator (Pozar, 2011) is given by

$$P_{in} = \tfrac{1}{2} VI^* = \tfrac{1}{2} Z_{in}|I|^2 = \tfrac{1}{2} Z_{in}|V/Z_{in}|^2 = \tfrac{1}{2} |I|^2(R+j\omega L - j1/\omega C) \tag{7}$$

The power loss in the series resistor R is given by

$$P_{loss} = |I|^2R \tag{8}$$

where I is current and R is resistance

The average magnetic energy stored in series inductor L is given by

$$E_m = \tfrac{1}{4} |I|^2L \tag{9}$$

The average electric energy stored in the series capacitor C is given by

$$E_e = 1/4|V_c|^2C = 1/4|I|^2 1/\omega^2C \tag{10}$$

where V_c is the voltage across the capacitor

The complex power in (7) can be rewritten as

$$P_{in} = P_{loss} + 2j\omega (E_m - E_e) \tag{11}$$

The input impedance in accordance with (6) is given by

$$Z_{in} = 2P_{in}/|I|^2 = [P_{loss} - 2j\omega (E_m - E_e) / (1/2|I|^2)] \qquad (12)$$

Resonance occurs when the average stored magnetic energy (E_m) and electrical energy (E_e) are equal such that $E_m = E_e$. The input impedance at resonance from (12) and (8) is given by

$$Z_{in} = P_{loss} / (1/2\ |I|^2) = R \qquad (13)$$

In accordance with (9) and (10), resonance occurs when $E_m = E_e$ such that the resonance frequency ω_o is given by

$$\omega_0 = 1/\sqrt{(LC)} \qquad (14)$$

Quality factor (Q) is given by

$$Q = (\omega \text{ average energy stored / energy loss per second})$$

$$= \omega (E_m + E_e) / P_{loss} \qquad (15)$$

Since Q is a measure of the loss of a resonance circuit, reduced loss implies a higher quality factor.

2.2 Conversion Loss

Conversion loss is another important consideration in mixer design and functionality. Conversion loss represents the resistive loss in the mixer and the losses due to frequency conversion process from the radio frequency (RF) to the intermediate frequency (IF) ports (Yang and Lin, 2015); (Shackeford, 1971); (Herold *et al*., 1945); (Jayasankar *et al*., 2024); (Kumara and Mondal, 2020); (Ali and Muttlak, 2025); (Pozar, 2011). Conversion loss is encountered in up-conversion and down-conversion processes. Conversion loss can be minimized by impedance matching at the three ports namely: radio frequency (RF), local oscillator (LO) and intermediate frequency (IF) ports such that the frequency/intermodulation products are absorbed by the resistive load or blocked by the reactive terminations of inductors and capacitors. Conversion loss of a mixer (L_c) is given by

$$L_c = [10 \log (\text{Available RF input power}) / (\text{Available IF output power})] \geq 0 \text{ dB} \qquad (16)$$

2.3 Noise Figure

In mixers, noise is often generated by diodes and transistors. In this paper, the noise figure is discussed in accordance with noise generated by the MOSFET transistors used in the mixer. The noise figure is dependent on if the input of the mixer is single side band (SSB) or double side band (DSB). The noise figure is more for DSB as the mixer will need to down convert at both sideband frequencies as both sidebands have the same intermediate frequency (IF) (Pozar, 2011). The power of single sideband is double that of double side band for the same amplitude. To illustrate the relation between the noise figure of SSB and DSB, the DSB input signal for lower side band (LSB) and upper side band (USB) is given by

$$V_{DSB}(t) = A\,[\cos(\omega_{LO} - \omega_{IF})t + \cos(\omega_{LO} + \omega_{IF})t] \quad (17)$$

where A is signal amplitude, ω_{LO} is local oscillator frequency and ω_{IF} is the intermediate frequency.
After mixing the DSB input signal with the LO signal $\cos\omega_{LO}t$ and passing through a low-pass filter, the down-converted IF signal is given by

$$V_{IF}(t) = AK/2\,\cos(\omega_{IF}t) + AK/2\,\cos(-\omega_{IF}t) = AK\cos\omega_{IF}t \quad (18)$$

where K is the constant representing the conversion loss for each band.

The average power of the DSB input signal (P_i) is given by

$$P_i = A^2/2 + A^2/2 = A^2 \quad (19)$$

where A is signal amplitude

Similarly, the average power of the IF output signal (P_o) is given by

$$P_o = A^2K^2/2 \quad (20)$$

Since the input noise power N_i is defined as

$$N_i = kT_0B \quad (21)$$

where k is Boltzmann's constant, T_0 is noise temperature (290K) and B is the IF bandwidth, the total output noise power (N_o) is the summation of the input noise and the noise added by the mixer (N_{add}) divided by the conversion loss (L_c) given by

$$N_o = [(kT_0B) + N_{add}] / L_c \quad (22)$$

From the definition of noise figure, the DSB noise figure of the mixer F_{DSB} is given by

$$F_{DSB} = (P_iN_o / N_iP_o) = [(2/ K^2L_c)\,(1 + N_{add}/kT_0B)] \quad (23)$$

where P_i is the average power of the input signal, N_o is the total output noise power, N_i is the input noise power, K is the constant accounting for the conversion loss for each side band, L_c is the conversion loss, N_{add} is the noise added by the mixer, k is Boltzmann constant, T_0 is the noise temperature in Kelvin and B is the IF bandwidth. In the case of single side band (SSB), the input signal is given by

$$v_{SSB}(t) = A\cos(\omega_{LO} - \omega_{IF})t \quad (24)$$

where A is the signal amplitude

After mixing the LO signal cosωLOt and passing it through a low-pass filter, the down-converted IF signal is given by

$$v_{IF}t = AK/2 \cos(\omega_{IF}t) \quad (25)$$

where K is the constant accounting for conversion loss.

The average input power of the SSB signal is given by

$$P_i = A^2/2 \quad (26)$$

The output average power of IF signal is given by

$$P_o = A^2K^2/8 \quad (27)$$

The input and output noise figures for SSB is given by

$$F_{SSB} = (P_oN_i / P_iN_o) = [(4/K^2L_c)(1 + N_{add}/kT_0B)] \quad (28)$$

Where FSSB is the input and output noise figure for SSB as every other parameter in (28) have the same definition as in (23).

The noise figure of mixer with SSB is twice the noise figure of mixer with DSSB such that

$$F_{SSB} = 2F_{DSSB} \quad (29)$$

3.0 MATERIALS AND METHOD

The mixer was designed using Keysight ADS BSIM_3 Model pMOS and nMOS MOSFET biased with drain supply voltage of 3V and gate voltage of 0V. Harmonic balance simulation was used whereby the local oscillator (LO) frequency was set at 700 MHz as the radio frequency (RF) was set at 800 MHz to sweep the drain resistance (R_D) for port-to-port isolation and conversion gain from 10 to 820 Ω at a step of 10 Ω giving a total of 82 points. The RF input power was set at 20 dBm. The circuit was terminated with a load resistance of 50 Ω. A combination of series and shunt lump components such as capacitors, inductors and resistors constitute the mixer input matching networks. In down-conversion, the RF port is the input while the IF port is the output. Whereas in up-conversion, the IF port is the input while the RF port is the output. The mixer block diagram showing the RF input voltage (V_{RFin}), LO input voltage (V_{LOin}) and the load voltage V_{load} is shown in Figure 6 while the mixer schematic circuit is shown in Figure 7.

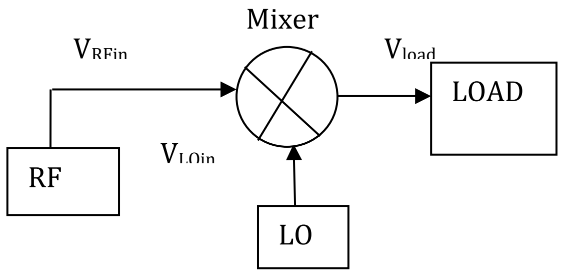

Figure 6: Mixer block diagram

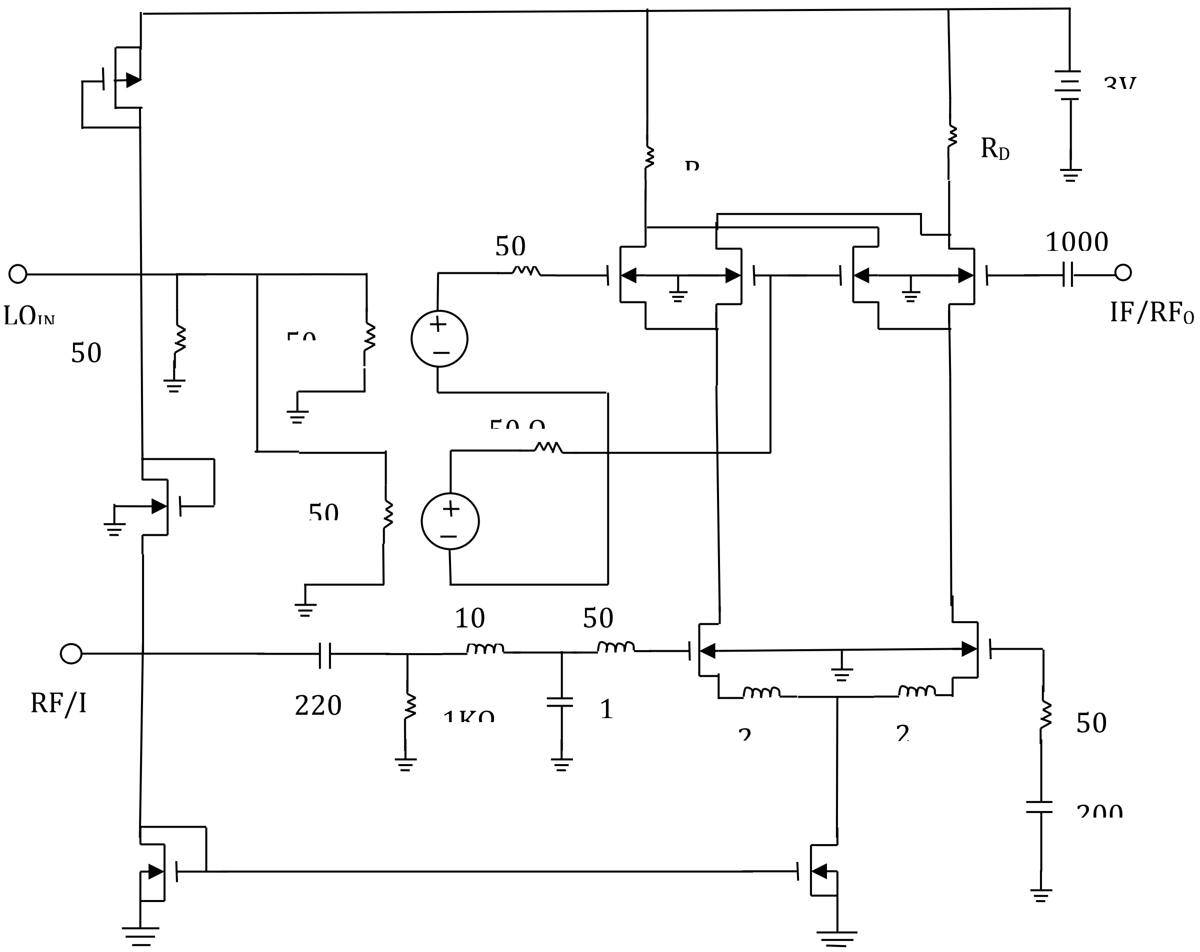

Figure 7: Mixer schematic circuit

4.0 RESULTS AND DISCUSSION

Harmonic balance simulation was carried out on the mixer and the RF frequency swept from 900 MHz to 1.5 GHz. The drain resistance RD was swept from 10 to 810 Ω.

In the first instance, the up/down conversion gain, port-to-port isolation, characteristic impedance (Zo), reflection coefficient and (Rho) and voltage standing wave ratio (VSWR) were calculated and shown in the respective figures and tables. In the second instance, the second and third order inter modulation frequency is shown and discussed.

4.1 Down/Up Conversion gain, port-to-port isolation, characteristic impedance (Zo), reflection coefficient (Rho) and voltage standing wave ratio (VSWR).

The drain resistance (R_D) swept during harmonic balance simulation from 10 to 820 Ω, indicates that at 410 Ω, the Up Conversion gain and Down Conversion gain are -4.50 dB and-1.98 dB respectively as shown in Figure 8. In Figure 9, the port-to-port isolation shows that at 410 Ω, the local oscillator (LO) to intermediate frequency (IF) denoted as LO2IF isolation is 52.02 dB. The local oscillator (LO) to radio frequency (RF) denoted as LO2RF isolation at 410 Ω is 68.83 dB. The radio frequency (RF) to intermediate frequency (IF) denoted as RF2IF isolation at 410 Ω is 16.57 dB. The power input (RF_{in}) and power output (IF_{load}) at 410 Ω when the drain resistance is swept from 10 to 820 Ω are -102.67 dBm and -58.97 dBm respectively as shown in Figure 10.

The tables showing the reflection coefficient (Rho), impedance and voltage standing wave ratio (VSWR) looking into the mixer RF(input) port, LO port and IF(output) port in Down Conversion and Up Conversion when the drain resistance is swept from 10 to 50 Ω are respectively shown in Tables 1, 2, 3, 4 and 5. Unlike in the mixer RF (input) port where there is a slight decrease in VSWR values as drain resistance increases from 10 to 50 Ω in Table 1, there is a marked decrease in VSWR values as the sweep parameter increases from 10 to 50Ω in Down Conversion and Up Conversion as shown in Tables 3 and 4 respectively. There is no reflection coefficient in local Oscillator (LO) port as shown in Table 2.

The Smith Chart showing the reflection coefficient (Rho) for RF (input), LO, IF (output) for Down Conversion and Up Conversion is shown in Figure 11.

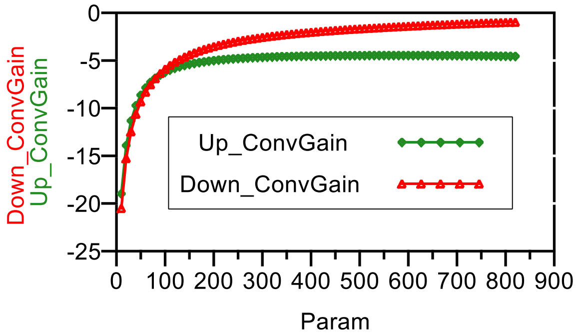

R_D(Ohms)

Figure 8: Conversion gain

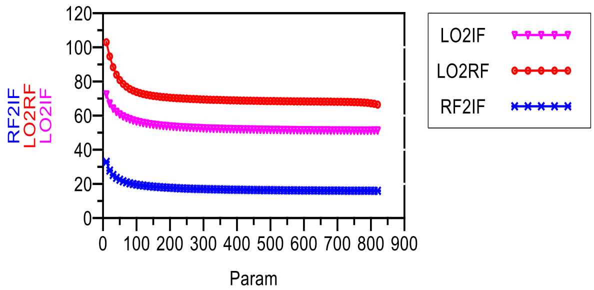

R_D(Ohms)

Figure 9: Port-to-port isolation

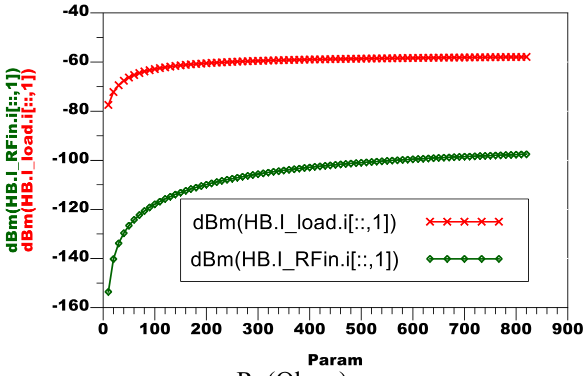

Figure 10: Input (RF) and Output IF Power

Table 1. Reflection Coefficient (Rho), Impedance and VSWR Looking into RF (Input) Port

Drain Resistance(Ω)	Reflection Coefficient	Impedance	VSWR
10	0.70/57.95	34.16+j79.39	5.66
20	0.70/57.93	34.21+j79.40	5.65
30	0.70/57.93	34.28+j79.38	5.65
40	0.70/57.93	34.28+j79.36	5.64
50	0.70/57.93	34.32+j79.32	5.63

Table 2. Reflection Coefficient (Rho), Impedance and VSWR

Drain Resistance(Ω)	Reflection Coefficient	Impedance	VSWR
10	0.00/0.00	50.00+j0.00	1.00
20	0.00/0.00	50.00+j0.00	1.00
30	0.00/0.00	50.00+j0.00	1.00
40	0.00/0.00	50.00+j0.00	1.00
50	0.00/0.00	50.00+j0.00	1.00

Table 3. Reflection Coefficient (Rho), Impedance and VSWR Looking into IF (Output) Port Down Conversion

Drain Resistance(Ω)	Reflection Coefficient	Impedance	VSWR
10	0.67/-175.95	10.00-j1.70	5.01
20	0.43/-174.51	19.99-j2.02	2.51
30	0.25/-170.94	29.97-j2.54	1.68
40	0.12/-59.83	39.93-j3.29	1.27
50	0.04/-89.45	49.36-j4.24	1.09

Table 4. Reflection Coefficient (Rho), Impedance and VSWR

Drain Resistance(Ω)	Reflection Coefficient	Impedance	VSWR
10	0.68/-176.49	9.68-j1.47	5.17
20	0.47/-166.45	18.10-j5.17	2.80
30	0.36/-149.87	24.66-j0.36	2.14
40	0.32/-130.47	29.29-j16.18	1.99
50	0.33/-113.97	32.22-j21.99	1.96

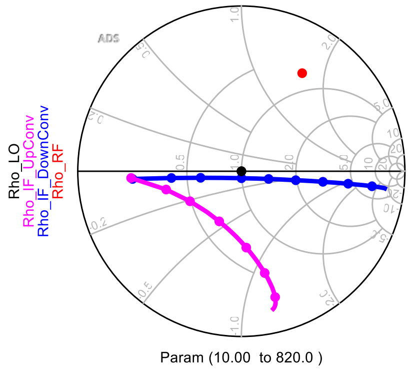

Figure 11. Reflection Coefficient (Rho) for RF, LO and IF (Down Conversion and Up Conversion)

4.2 Fundamental Output Power for lower Sideband and Upper Sideband and Third Order Intermodulation (IM3) Power in the Lower Sideband (LSB) and Upper Sideband (USB).

The fundamental output power (IF) for lower sideband (LSB) and upper sideband (USB) versus input frequency swept from 900 MHz to 1.5 GHz. At centre frequency of 1.2 GHz, the low referred third order intercept (TOI_low) is -8.54 dBm while the high referred third order intercept power (TOI_high) is 10.59 dBm as the transducer power gain is -25.63 dB as shown in Figure 12. The IF (output) power at lower sideband (IF_LSB) and IF (output) power at upper sideband (IF_USB) at 1.2 GHz centre frequency are respectively -55.63 dBm and -55.64 dBm as the third order intermodulation power for lower side band (IM3_LSB) and the third order intermodulation power for the upper sideband (IM3_USB) are -98.56 dBm and -136.86 dBm respectively as shown in Figure 13.

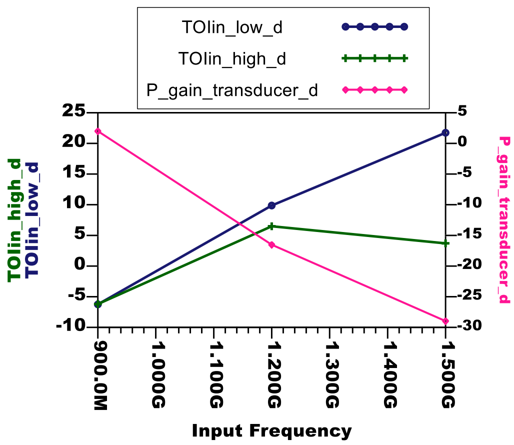

Input Frequency (GHz)

Figure 12: Referred third order intercept power and transducer power gain from 900 MHz to 1.5 GHz

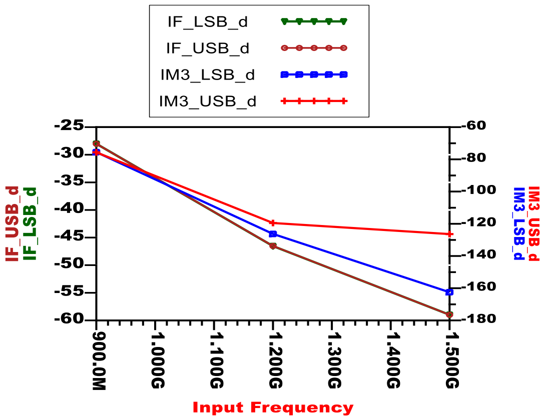

Input Frequency (GHz)

Figure13: IF and IM3 power for lower and upper side bands from 900 MHz to 1.5 GHz

5.0 CONCLUSION

A 900 to 1.5 GHz Single-ended CMOS Mixer for wireless communication has been proposed, designed simulated and presented. Harmonic balance simulation has been used to sweep the drain resistance and fundamental frequency from 900 MHz to 1.5 GHz. The Conversion gain, port-to-port isolation, referred high and low third order intercept power as well as third order intermodulation power for the lower and upper sidebands have been presented and discussed. The mixer will find applications in wireless communication systems operating from 900 MHz to 1.5 GHz.

REFERENCES

Ali, M. R. & Muttlak, S. (2025). Design and Simulation of 26.8 GHz Sub-Harmonic Mixer for 5G Mobile System Applications. Proceedings of 5th International Conference on Scientific Innovative Studies, Konya, Turkey.

Boeck, R., Jaeger, N. A. F., Rouger, N. & Chostowski, L. (2010). Series-Coupled Silicon Racetrack Resonators and the Venier Effect . Optics Express, 18(24), 25151-25157.

Chen, Z., Zhang, B., Yong, F. & Yuan, Y. (2016). 190-240 GHz Subharmonic Mixer Based on 3D Geometric Modelling of Schottky Diodes and CAD Load-Pull Techniques. IEICE Electronics Express, 13(16), 1-9.

Chong, W. K., Ramiah H., Vitee, N. & Tan, G. H. (2014). Design of Inductorless, Low power, High Conversion Gain CMOS Subharmonic Mixer for 2.4 GHz Application. 2014 IEEE International Microwave and RF (IMaRC) Conferences, Bangalore, India, 274-277.

Danndsena, J. & Jena, D. P. (2022). Wave Propagation Through Resonators, Resonators in Series and Multi-Resonator. Wave Dynamics, World Scientific Publishing Co, USA, 181-191.

Jayasankar, D.,Reck, T., Durant, S., Stake, J. & Hesler, J. (2024). A Broadband Conversion Loss Measurement Techniques for Terahertz Harmonic Mixers. IEEE Transactions on Terahertz Science and Technology, 14(3), 424-427.

Kishokumar G., Muralitharian, S., Elalasingham, G. A. R., Arumprasanth, S., Narampanawe, K. M. M. W. N. B. & Gunawardena, A. U. A. W. (2011). Microwave Mixer Design to Extend the Measurement Range of Spectrum Analyser. Annual Transaction of IESL, 533-539.

Kumari, S. & Mondal, P. (2020). A Low Conversion Loss Single Balanced Loss Single Balanced Subharmonic Mixer. International Journal of RF and Microwave Computer Aided Engineering, 30(5), 1-7.

Lin, Y. W., Lee, S., Ren,Z., & Nguyen C. T. C. (2003). Series-Resonant Micro Mechanical Resonator Oscillator. IEEE Electron Devices Meeting, Washington DC, USA, 39.4.1-39.4.4.

Lugo-Hernandez, E., Mirea, T., Carmona, J. M., Clement, M., Olivares, J., Collado, J. C., Mateu, J. (2023). Analysis of Spurious Peaks at Series Resonance in Solidly Mounted Resonators by Combined BVD-Mason Modelling. Ultrasonics, 131, 106958.

Marki, F. & Marki, C. (2018). Mixer Basics and Primer, A Tutorial for RF and Microwave Mixers. Microwave Journal, 2.

Mudjar, A. & Musia, M. (1993). Design and Performance of x4 Millimeter wave Subharmonic Mixer. 23rd European microwave Conference, Madrid, Spain, 46-247.

Pozar, D. M. (2011). Microwave Engineering, Fourth Edition, Wiley and Sons Inc. , USA, 637-652.

Seyedhosseinzadeh, N. & Nabavi, A. (2017). Design of an Active CMOS Subharmonic Mixer with Enhanced Transconductances. AEU-International Journal of Electronics and Communication, 73, 98-104.

Wang, H., Rollin, J. M., Davies, S. R. & Maestrini, A, (2006). Design of a Low-Noise Integrated Subharmonic Mixer at 183 GHz using European Scottky Diode Technology. Proceedings of 4th ESA Workshop Technology and Applications.

Wen, J., Zhang, S., & Lingling, S. (2020). A Compact Broadband Monolithic Sub-Harmonic Mixer Using Multi-Line Coupler. MDPI Journal of Electronics, 9(4), 694.

Weng, R. M., Wang, J. C. & Li, S. Y. (2007). A Low Power Folded Mixer Using Even Harmonic Technology, IEEE International Workshop on Radio Frequency Integration Technology.

Yang, N., Chen, Z. N, Qing, X. M. & Guo Y. X. (2005). Serially-Connected-Series-Stub Resonators and their Applications in Coplanar Stripline Bandpass Filter Design. IEEE MTTS International Symposium Digest, Long Beach, CA, USA, 695-698.